ISBN: 978-3-95450-231-8 ISSN: 2673-5490 doi: 10.18429/JACoW-IPAC2023-MOPA110

PRECISE CONTROL OF A STRONG X-Y COUPLING BEAM TRANSPORTATION FOR J-PARC Muon g-2/EDM EXPERIMENT*

H. Iinuma†, Ibaraki University, Mito, Japan
M. Abe, K. Sasaki, H. Nakayama, T. Mibe[1], KEK, Tsukuba, Japan
S. Ogawa, T. Yamanaka, Kyushu University, Fukuoka, Japan
Y. Sato, Niigata University, Niigata, Japan
[1] also at Tokyo University, Tokyo, Japan

Abstract

In this study, a strategy for designing a dedicated beam injection and storage scheme for the J-PARC Muon g-2/EDM experiment is described. To accomplish a three-dimensional beam injection into the MRI-type compact storage system, transverse beam phase spaces (so-called X-Y coupling) should be coupled appropriately. A pulsed kicker system is a key to control vertical motion inside the storage volume. Moreover, dedicated beam phase control through the *beam channel* of the storage magnet's yoke is crucial. We introduce five-dimensional phase-space correlation in addition to a strong X-Y coupling, to control stored vertical beam size as small as a level of one-third.

INTRODUCTION

A new measurement of the muon's anomalous magnetic moment $a_\mu = (g-2)/2$ and its electric dipole moment (EDM) is in preparation at the J-PARC muon facility at MLF, MUSE [1]. These physics quantities are suitable probes for exploring beyond the standard model in elementary physics. Experimentally, we measure them from a difference of two angular frequencies of spin procession frequency and the orbital cyclotron frequency in a homogeneous magnetic field but no electric field, as Eq. (1).

$$\vec{\omega} = -\frac{q}{m}a_\mu \vec{B} + \frac{\eta}{2}\left(\vec{\beta}\times\vec{B}\right) \quad (1)$$

Here, two dipole moments of the muon are introduced:

$$\vec{\mu}_\mu = -\frac{gq}{2m}\vec{s},\ \vec{d}_\mu = \eta\frac{q}{2mc}\vec{s}, \quad (2)$$

and, c and q are the speed of light and a unit charge, and m and g are the mass and gyromagnetic ratio of the muon, respectively. If we assume non-zero η here, but assuming that $\vec{\beta}\cdot\vec{B} = \vec{\beta}\cdot\vec{E} = 0$, the first term in equation 1, which express a muon magnetic moment, is orthogonal to the second which includes the EDM related term η, required to be extremely small from the standard model. Tilt angle of ω to $\vec{B}$ is proportional to the magnitude of the EDM and is of the order of 1 mrad, considering the upper limit from the previous experiment E821 [2] ($|\vec{d}_\mu| = 0.9\times10^{-19}\ e\cdot\mathrm{cm}$). To achieve a 100-times better sensitivity, we should be sensitive to 0.01 mrad.

* Work supported by JPS KAKENHI Grant Numbers JP19H00673 and JP20H05625.
† hiromi.iinuma.spin@vc.ibaraki.ac.jp

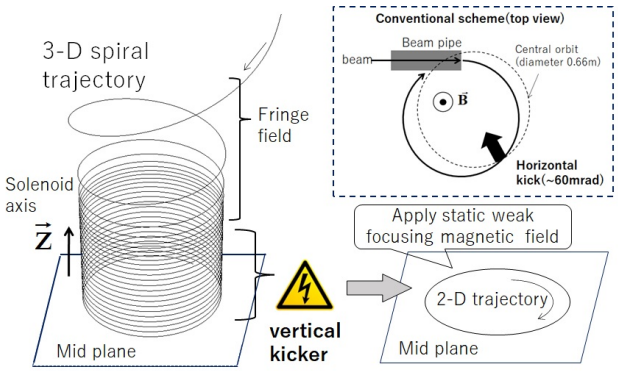

Figure 1: Outline of three-dimensional spiral injection scheme [1,3].

In J-PARC, a slow muon source and muon LINAC technology have been developed [1] to have a low emittance muon beam of momentum of 300 MeV/c. Thereafter, muons are stored in a 3 T storage volume, the diameter of the orbital cyclotron motion becomes *only* 0.66 m. This is the smallest storage ring for relativistic energy beams in the world. To realize this technical challenge, a new beam injection scheme called the **three-dimensional spiral injection scheme**, as shown in Fig 1, are being developed [3]. The beam enters the solenoid through a channel in the top iron yoke 110 cm above the storage volume (refer to Fig. 2) and its spiral motion is compressed by the *Fleming force* owing to the static radial field (B_R). A vertical kick (pulsed radial magnetic field) is applied to store the beam on arrival to the storage region. A small static weak-focusing field in the fiducial volume maintains the beam in the storage region.

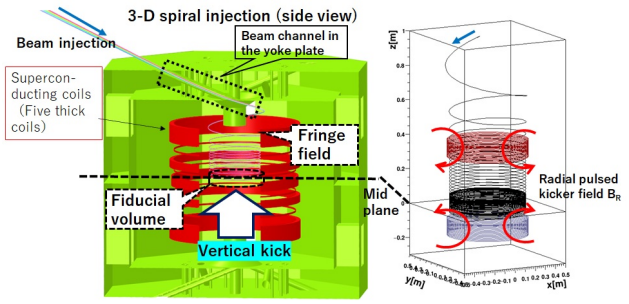

Figure 2: Superconducting solenoid magnet and kicker coils [1,4].

ISBN: 978-3-95450-231-8 ISSN: 2673-5490 doi: 10.18429/JACoW-IPAC2023-MOPA110

VERTICAL BEAM MOTION CONTROL BY PULSED KICKER

Relation of a single track motion and a time structure of a pulsed kicker current will be introduced. Details of design concept of kicker coil shape are discussed in Ref. [5].

A Single Track Motion Controlled by Pulsed Kicker

Figure 3 shows vertical position of single track as a function of time. Effective magnetic field along the trajectory is also shown. We employ a half-shine shaped kicker pulse with $T_K = 120$ ns duration time.

$$\begin{aligned} I(t) = & \quad I_0 sin\Big(\frac{\pi}{T_K}(t-t0)\Big), : (t-t_0) < T_K \\ = & \quad 0, : (t-t_0) > T_K \end{aligned} \tag{3}$$

Effective radial field along a single track is

$$\begin{aligned} B_R(z,R,t) = & \quad B_R^{static}(z,R) \\ & + B_R^{kicker}(z,R) sin(\frac{\pi}{T_K}(t-t0)). \end{aligned} \tag{4}$$

A correlation of vertical potions and pitch angles along the trajectory is also shown. Role of vertical pulsed kicker is to guide trajectory for both vertical position and pitch angle are zero when kick current back to zero. There is a freedom to design trajectory during the kick period, depends on kicker coil shape and kicker duration time and current as long as integrated $B_R L$ along the trajectory satisfies Eq. (5) [5].

$$BL = \int B_R(z,R,t)dl. \tag{5}$$

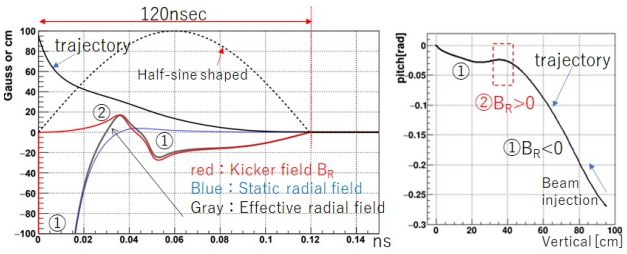

Figure 3: Left:Vertical motion of a single track as a function of time. Right: Correlation of vertical position and pitch angle.

Multi Beam Motion Expecting Beam Phase Space

Now we consider expected beam phase space and see how trajectories of particle differ as shown in Fig. 4.

Without change kicker coil shape, but shorter T_K and bigger I_0 case, vertical beam beam distribution after the kick is well controlled.

To meet experimental requirement, smaller vertical beam distribution $|z|$ after the kick is favored. Trajectories in red lines corresponds to $|z| < 3$ cm, which indicate ideal bean injection and storage. On the other hand, black lines are stored inside the weak focusing magnetic field but $|z| < 10$ cm. By

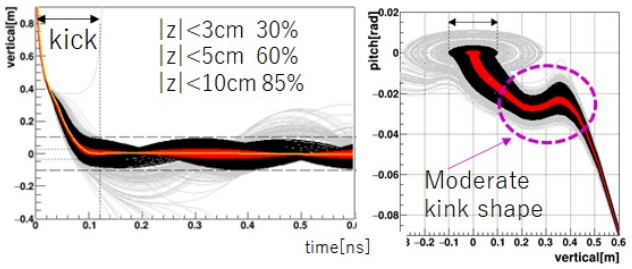

Figure 4: Beam motion with expected phase space with moderate kicker parameter [5].

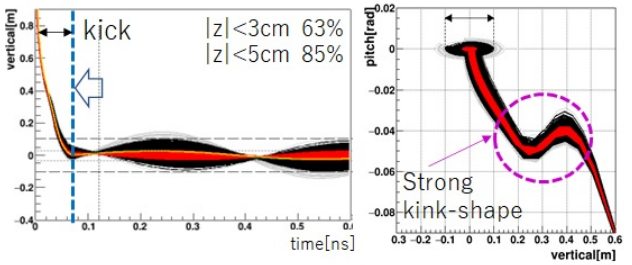

Figure 5: Beam motion with expected phase space with strong kicker parameter for trials calculation.

comparing Figs. 4 and 5, the shorter T_K and bigger I_0 have big advantage to control $|z|$. This is because stronger kick has stronger vertical focusing field as clear in *kink shape*. However, it costs high voltage on the kicker coils of $V > 80$ kV, which may cause severe technical difficulties for kicker's conductor design. Therefore, strong kicker case of Fig. 5 is not realistic solution. In order to stay with $V < 30\ kV$, we need to consider how beam phase space should be controlled from Fig. 4 trajectories.

Vertical Phase Space and Integrated $B_R L$

Left plots of Figs. 6 and 7 show time slice of vertical phase space at the end of the kick. Integrated $B_R L$ distributions are also shown in the right.

From these plots, stronger kick can control $B_R L$ better. This is very consistent that *kink shape* in Fig. 5 is stronger than that of Fig. 4.

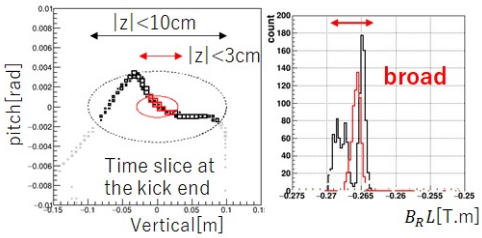

Figure 6: Time sliced vertical phase space at the end of the moderate kick and $B_R L$ distribution. Red corresponds to $|z| < 3$ cm. Closed ellipses are from weak focusing field [5].

ISBN: 978-3-95450-231-8 ISSN: 2673-5490 doi: 10.18429/JACoW-IPAC2023-MOPA110

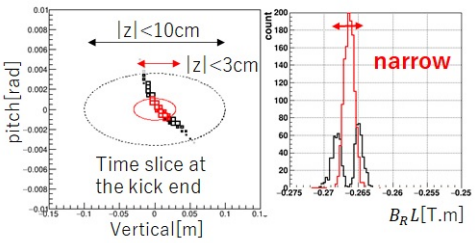

Figure 7: The same plots as Fig. 6 but for the strong kick.

BEAM PHASE SPACE STUDY

Staying with high voltage at kicker coil $V < 30$ kV, how do we realize smaller $|z|$ distribution? We studied beam phase space by use of three parameters: $|r|$, θ and vertical distributions z_g which are from six components of each trajectory in global coordinate system.

$$\begin{aligned} \vec{r} &= (x_g, y_g, z_g),\ \vec{p} = (p_x, p_y, p_z) \\ |r| &= \sqrt{x_g^2 + y_g^2 + z_g^2},\ cos(\theta) = \frac{\vec{r}\cdot\vec{p}}{|r||p|} \end{aligned} \tag{6}$$

Figure 8 shows correlations of these three parameters at different positions along the beam injection trajectory.

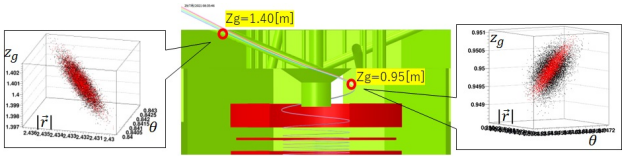

Figure 8: Zoom up view of *channel* in the yoke. $|r| - \theta - z_g$ correlation at different points are also shown.

Red and black distributions, as introduced previous section, are separated at $z_g \sim 0.95$ m (inside the storage magnet's yoke), however, *not* for $z_g \sim 1.40$ m (entrance point of the *channel* in the storage magnet's yoke). It seems that three parameters are not enough to distinguish red and black sub-groups.

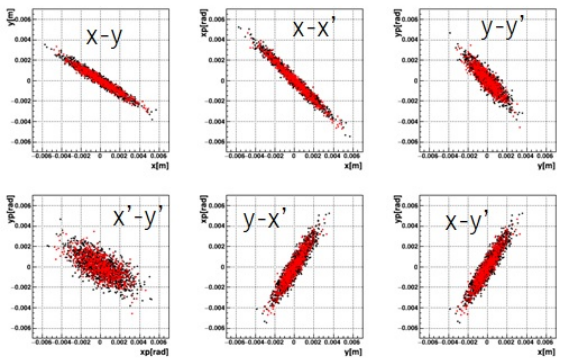

Figure 9: X-Y coupling in the beam frame, at the injection point, controlled in the upstream beam transport line [6].

Upstream beam transport line [6] is dedicated to control so-called X-Y coupling in the beam frame, at the injection point, as in Fig. 9. However, there is no obvious hint indicating how to control beam phase space to achieve $|z| < 3$ cm.

Correlation Finding With Five Phase Space Parameters Through the Channel

Each beam trajectory has six phase space parameters, but it is fair to set five are independent, because we can treat as beam momentum is fixed.

In addition to Eq. (7), we invite another two angles:

$$sin(\psi) = \frac{p_z}{|p|},\ cos(\phi) = \frac{p_x}{\sqrt{{p_x}^2 + {p_y}^2}}. \tag{7}$$

And then, we define $n \times 5$ matrix: $\mathcal{M}_{red}$ as

$$\mathcal{M}_{red} = \begin{pmatrix} |\vec{r_0}| - \bar{r} & \theta_0 & z_{g0} - \bar{z_g} & \psi_0 & \phi_0 \\ |\vec{r_1}| - \bar{r} & \theta_1 & z_{g1} - \bar{z_g} & \psi_1 & \phi_1 \\ \vdots & \vdots & \vdots & \vdots & \vdots \\ |\vec{r_n}| - \bar{r} & \theta_n & z_{gn} - \bar{z_g} & \psi_n & \phi_n \end{pmatrix} \tag{8}$$

here, n is number of red-subgroup's trajectories. $\bar{r}$, $\bar{\theta}$, $\bar{z_g}$, $\bar{\psi}$ and $\bar{\phi}$ are mean values of red-subgroup in Fig. 8. We apply singular value decomposition on $\mathcal{M}_{red}$, and obtain an eigen vector of the smallest eigen value:

$$\vec{q} = (q_r, q_\theta, q_z, q_\psi, q_\phi). \tag{9}$$

Now, we define $N \times 5$ matrix:$\mathcal{M}_{tot.}$ of all trajectories, and estimate vector $\vec{d} = \mathcal{M}_{tot.}\vec{q}$. Total N components of $\vec{d}$ are residues and indicate how differ red and black sub-groups as in lower histograms in Fig. 10.

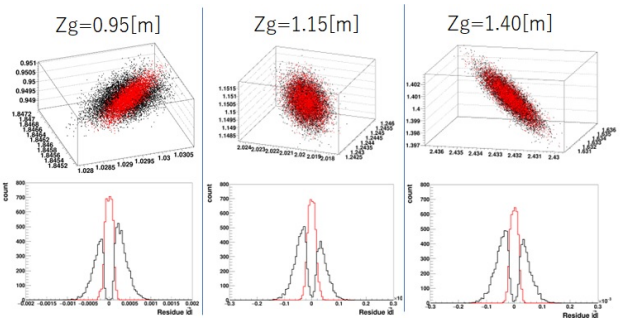

Figure 10: Upper:$|r| - \theta - z_g$ correlations do not help to distinguish red and black groups. Lower:Residue vector $\vec{d}$ components indicates a way of precise beam phase control.

CONCLUSION AND NEXT

Besides strong X-Y coupling, five-parameter phase space correlation should be consider to control precise vertical beam motion in the storage volume. Based on this study, specification of additional multipole magnet at the injection point is now under considering.

ISBN: 978-3-95450-231-8 ISSN: 2673-5490 doi: 10.18429/JACoW-IPAC2023-MOPA110

REFERENCES

[1] M. Abe and J-PARC g-2/EDM Collaboration, "A new approach for measuring the muon anomalous magnetic moment and electric dipole moment", *Prog. Theor. Exp. Phys.*, vol. 2019, p. 053C02, 2019. doi:10.1093/ptep/ptz030

[2] G. W. Bennett *et al.*, (Muon (g-2) Collaboration) "Improved limit on the muon electric dipole moment", *Phys. Rev. D*, vol. 80, p. 052008, 2009. doi:10.1103/PhysRevD.80.052008

[3] H. Iinuma *et al.*, "Three-dimensional spiral injection scheme for g-2/EDM experiment at J-PARC", *Nucl. Instrum. Meth. Phys. Res. Sect. A*, vol. 832, pp. 51–62, 2016. doi:10.1016/j.nima.2016.05.126

[4] M. Abe *et al.*, "Design method and candidate of a magnet for muon g- 2/EDM precise measurement in a cylindrical homogeneous volume", *Nucl. Instrum. Meth. Phys. Res. Sect. A*, vol. 890, pp. 51–63, 2018. doi:10.1016/j.nima.2018.01.026

[5] H. Iinuma *et al.*, "Design work of pulsed radial kick field for J-PARC muon g-2/EDM experiment", in *Proc. PASJ2022*. https://www.pasj.jp/web_publish/pasj2022/proceedings/PDF/TUP0/TUP036.pdf

[6] H. Iinuma, H. Nakayama, M. Abe, K. Sasaki, and T. Mibe, "Design of a Strong X-Y Coupling Beam Transport Line for J-PARC Muon g-2/EDM Experiment", *IEEE Trans. Appl. Supercond.*, vol. 32, no. 6, pp. 1–5, Sep. 2022. doi:10.1109/TASC.2022.3161889